ISBN: 978-3-95450-241-7 ISSN: 2673-5350 doi:10.18429/JACoW-IBIC2022-MO3C2

DIAMOND-II ELECTRON BEAM POSITION MONITOR DEVELOPMENT

L. T. Stant*, M. G. Abbott, L. Bobb, G. P. Cook, L. Hudson,
A. F. D. Morgan, E. Perez-Juarez, A. J. Rose, A. Tipper
Diamond Light Source, Oxfordshire, United Kingdom

Abstract

The UK national synchrotron facility, Diamond Light Source, is preparing for a major upgrade to the accelerator complex. Improved beam stability requirements necessitate the fast orbit feedback system be driven from beam position monitors with lower noise and drift performance than the existing solution. Short-term beam motion must be less than 2 nm/$\sqrt{\text{Hz}}$ over a period of one second with a data rate of 100 kHz, and long-term peak-to-peak beam motion must be less than 1 µm. A new beam position monitor is under development which utilises the pilot-tone correction method to reduce front-end and cabling perturbations to the button signal; and a MicroTCA platform for digital signal processing to provide the required data streams. This paper discusses the challenges faced during the design of the new system and presents experimental results from testing on the existing machines.

INTRODUCTION

Diamond Light Source is a 3 GeV, 300 mA third-generation synchrotron located in Oxfordshire, UK. User operation began in early 2007 and since then a total complement of 33 beamlines have been commissioned. To further increase capabilities of the facility a new injector and storage ring will replace the existing machine, with the 18-month dark period scheduled for late 2026. This major upgrade, Diamond-II, will increase the energy to 3.5 GeV, reduce the horizontal emittance to 160 pm, and provide twice the number of straights [1].

As part of the Diamond-II upgrade, the storage ring electron beam position monitor (EBPM) processing electronics will be replaced[1]. Several factors influenced this decision:

- Due to the higher closed-loop crossover frequency and lower latency requirements of the fast orbit feedback for Diamond-II, the data rate from the EBPM system must increase from 10 kHz to 100 kHz, which is not supported by the existing systems.
- At the time of the Diamond-II CDR [1], the state-of-the-art multiplex switching solution would have created many harmonics in the measurement data for the required data rate.
- The existing systems will be over 20 years old and most have been repaired at least once.

Table 1 summarises the requirements of the Diamond-II EBPM system.

Table 1: EBPM Requirements for Diamond-II

Parameter	Diamond-II
Number of EBPMs	252 (11/12 per cell)
Geometric factor k	7.3 mm
Short-term motion (<1 s)	
Commissioning (0.3 mA)	<130 nm/$\sqrt{\text{Hz}}$
User beam (300 mA)	<2 nm/$\sqrt{\text{Hz}}$
Long-term motion (<1wk)	<1 µm pk-pk

The increasing adoption of the MicroTCA computing platform in the synchrotron community, combined with suitable technical resource available at Diamond Light Source, led to the choice of an in-house developed solution instead of an off-the-shelf product. The different parts of the EBPM system design will now be discussed.

BUTTON PICKUPS

Similar to Diamond, there will be two types of EBPM: primary EBPMs used for insertion device beam alignment will be located in straights on dedicated thermally stable pillars; and standard EBPMs located in the arcs will be mounted directly to the girders. Whereas the Diamond vessels were significantly wider in the horizontal dimension, the Diamond-II vessels are circular.

The button pickups are of a similar design to those used in the Diamond DDBA cell upgrade [2] and the ESRF design [3]. Due to the challenging manufacturing requirements of the button pickups, ongoing discussions with suppliers and other light sources have been necessary [4].

FRONT-END SYSTEMS

Analogue Front-End

Before digitisation, the signal from the button pickups must be filtered and amplified/attenuated by an analogue front-end. Typically, this unit will also include some form of compensation scheme to continuously correct the gain and phase variations between the EBPM channels. In Diamond, the compensation scheme chosen was multiplex switching located outside the vault. By moving the compensation inside the vault (i.e. closer to the buttons) it is possible to also correct for variations in cable gain and phase which have been shown to vary with temperature and humidity [5]. Due to promising results [6–9] and the avoidance of switching harmonics, the pilot tone compensation scheme was selected for use in the Diamond-II analogue front-end (D2AFE).

The D2AFE module (shown in Fig. 1a) contains four RF channels, each comprising of two stages of filtering, ampli-

* laurence.stant@diamond.ac.uk

[1] The existing LINAC and booster EBPM systems will be refurbished and upgraded as a future project.

ISBN: 978-3-95450-241-7 ISSN: 2673-5350 doi:10.18429/JACoW-IBIC2022-MO3C2

fication and switched attenuation as shown in Fig. 2. An externally supplied pilot tone is coupled into the channel as early as possible, to compensate for variation in the D2AFE components. Helical filters are used for the bandpass elements. Channel performance of the current prototype is 52 dB maximum gain, >80 dB spurious-free dynamic range, 14 MHz bandwidth and −51 dB adjacent channel crosstalk. An output power measurement is provided via a coupler and log detector, which can trigger a <500 ns trip to engage full attenuation and protect downstream equipment.

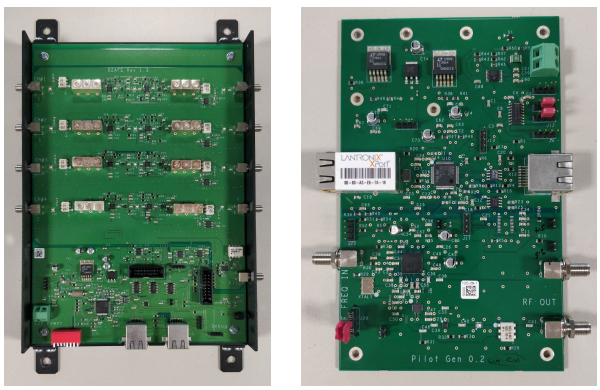

(a) D2AFE. (b) PTG.

Figure 1: The PCB assemblies for the front-end systems. The D2AFE board size is 17 cm by 24 cm and the PTG board size is 10 cm by 16 cm.

Control of the switched attenuation and monitoring of power supplies, RF output powers and temperatures is provided per cell via a chained RS485 serial interface over Cat6 cable to the Controls Instrumentation Area (CIA) outside the vault. Power for each cell is provided via dual-redundant 12 V switched-mode supplies in the CIA, individually cabled to each D2AFE where linear regulators provide quiet 5 V and 3.3 V rails.

To validate the decision to locate the D2AFEs on the girder, radiation measurements have been taken over the previous two years. A set of RADFET [10] sensors and D2AFE boards have been located on the side of the girder downstream of the storage ring injection septum and collimators. Table 2 lists the measured doses, with negligible exposure on or close to the floor of the vault. A survey of radiation tolerance of D2AFE parts showed the only concerning items were the linear regulators, which degraded after a 40 Gy dose on a board mounted to the beampipe. The STM32 ARM microcontroller has shown no operational issues up to 170 Gy. The lower girder positions should receive a dose of 40 Gy after only 3.3 years with Diamond-II predicted losses, so instead D2AFEs will be located as close to the floor as possible. Extra noise and drift from the longer cables before pilot injection will be alleviated using passive external pilot injectors mounted on the girder top, connecting to the buttons using semi-rigid cable.

Table 2: Radiation Measurements over Two Years beside Diamond Girder, Downstream of Injection (Highest Dose Area)

Position	Radiation Dose (Gy)
Beampipe	308
100 mm below girder top	7.7
200 mm below girder top	5.4
300 mm below girder top	3.2
400 mm below girder top	4.0
500 mm below girder top	Negligible
Floor of vault	Negligible

Pilot Tone Generator

A single pilot tone is generated per cell by a redundant pair of pilot tone generators (PTG, shown in Fig. 1b) located in the CIA, and is distributed to a maximum of 16 D2AFEs. The tone is generated by a dual-loop PLL locked to a machine RF reference from an event receiver, avoiding the risk of free-running local crystals struggling with the narrow pilot filter in digital processing. The two modules feed an RF hybrid which allows the running PTG to failover to the backup without swapping hardware. Each output routes to one of the two cell girders, where at a patch panel another D2AFE unit is used as a distribution amplifier with controllable attenuation per channel (with pilot input terminated). These outputs are then distributed to the D2AFEs along the girder via local two-way splitters.

The PTG also provides the RS485 to Telnet interface for the D2AFE serial chain, which is available to the MicroTCA EPICS IOC in the same rack. Each end of the RS485 chain connects to a PTG, to provide separate redundancy of both the control interface and pilot tone. The PTG and D2AFE use a similar ARM microcontroller with common libraries for communication and firmware updates.

Firmware Update Method

To update nearly 300 D2AFEs and PTGs using local programming adapters would be very inefficient, so a remote firmware update method was developed using an in-application bootloader. This method can update the entire storage ring in under ten minutes if required, as each cell can run updates in parallel. In case a bad firmware is deployed, a fast handheld programmer with rescue image is being prepared to minimise disruption.

DIGITISATION AND PROCESSING

The EBPM signals from the entire cell are brought to a diagnostics rack in the CIA. A single 12-slot MicroTCA chassis, shown in Fig. 3, contains all of the required AMC cards for EBPMs, x-ray beam position monitors (XBPM), receiving machine events and providing machine protection outputs from beam position interlocks. For Diamond-II the orbit feedback and beamline interlocks will also include XBPM data to improve drift and fault tolerance, so it is

ISBN: 978-3-95450-241-7 ISSN: 2673-5350 doi:10.18429/JACoW-IBIC2022-MO3C2

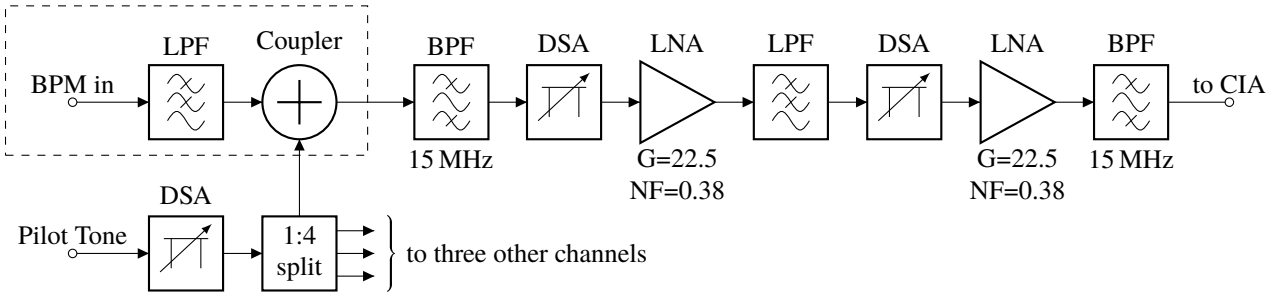

Figure 2: The architecture for one of the four channels in the D2AFE unit, including low-pass filters (LPF), helical band-pass filters (BPF), digital step attenuators (DSA) and low noise amplifiers (LNA). The initial filter and coupler (dotted box) is being developed as an external option.

convenient to locate them together and standardise on the same FMC carrier AMC. Each EBPM digitiser card uses two 8-channel 16-bit 250 Msps ADC FMCs, allowing for four EBPMs per card. This means a maximum provision of 16 EBPMs can be facilitated with only four AMCs. Beam position interlocks can be provided for the machine protection system using a custom RTM connected to one or more of the EBPM AMCs, subject to implementation.

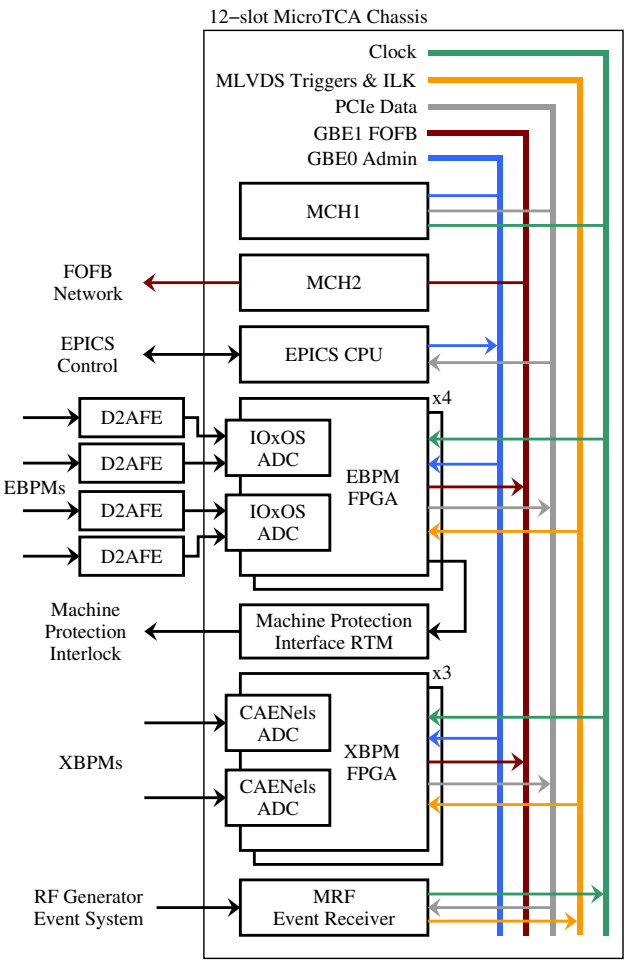

Figure 3: Architecture of a cell diagnostics MicroTCA crate.

The ADC data, acquired at 215 Msps, can be streamed directly to RAM for development and testing, but otherwise is mixed with a 70 MHz reference ($f_{RF} - 2f_{sample}$) before downsampling into standard acquisition streams, as shown in Fig. 4. In addition to the fast and slow acquisition (FA, SA) streams, a medium acquisition (MA) stream is generated for use in fault detection. The pilot signal is extracted as additional FA, MA and SA streams for analysis.

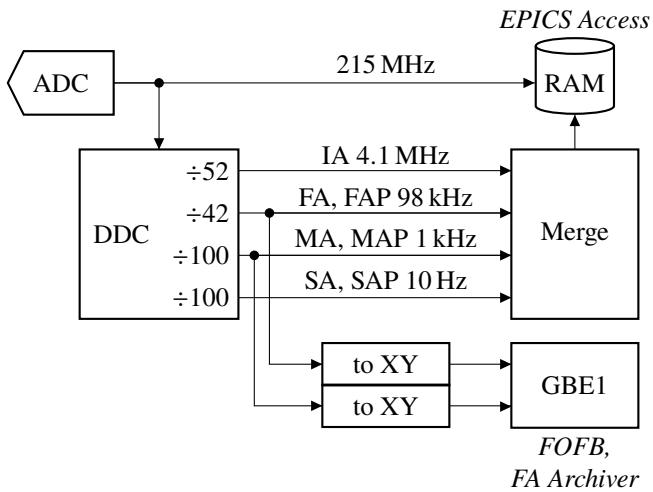

Figure 4: Diamond-II EBPM data streams. The fast, medium and slow acquisition streams also generate respective pilot streams.

SYSTEM MEASUREMENTS

A spare EBPM on the Diamond storage ring has been used for testing the design. The majority of testing so far has been to assess noise and drift performance, using a 1:4 splitter driven by a single button pickup. Figure 5 shows an SA measurement of this setup, which highlights the benefit of a pilot-compensated signal. The line at 1.67 mHz and its decaying harmonics are caused by the 10 minute top-up, and are reduced by increasing the attenuation in the D2AFE to improve the linearity. This is a trade-off with signal-to-noise ratio and is still under investigation. The line at 0.5 Hz is the flash rate of a status LED on the D2AFE modulating the

ISBN: 978-3-95450-241-7 ISSN: 2673-5350 doi:10.18429/JACoW-IBIC2022-MO3C2

power supply, which shows the high system sensitivity. This status LED has now been made steady-state.

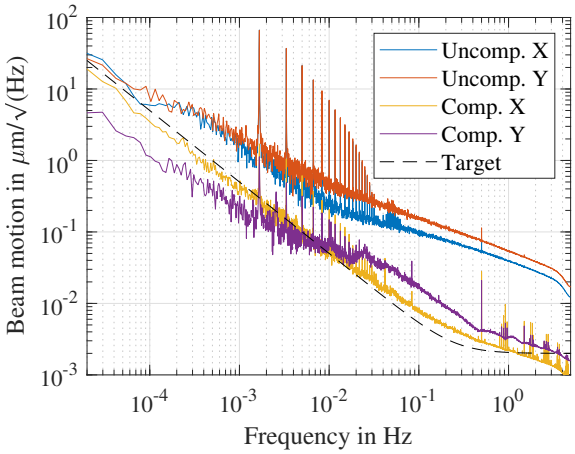

Figure 5: Spectral plot of EBPM motion from SA stream. Target is the <2 nm/$\sqrt{\text{Hz}}$ short-term requirement blended towards the <1 µm pk-pk long-term requirement below 1 Hz.

Increased noise on the Y signal is caused by the FMC ADC arrangement. Each ADC has two channels, so a four-button EBPM will have two groups of two channels with correlated noise, with uncorrelated noise between groups. The ABCD-to-XY transformation means that either X or Y will have improved noise, so the cables will be reconfigured to optimise the vertical Y signal.

Figure 6 shows an equivalent measurement from the FA stream. Although there are some spectral lines still to investigate, the performance is generally well within the requirement.

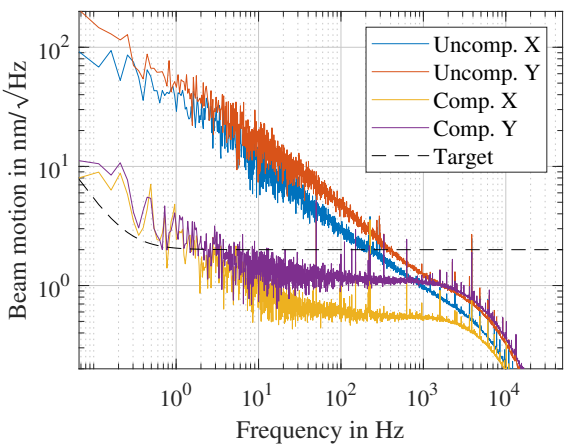

Figure 6: Spectral plot of EBPM motion from FA stream. The target continues as for Fig. 5.

Stability measurements from the SA stream are shown in Figs. 7 and 8. Although the performance of the Y signal is satisfactory, the X signal is drifting significantly, at times exceeding the target. The cause of this is revealed in Fig. 8, where the C and D button signals are shown to be strongly correlated with humidity measured close to the EBPM. Some humidity correlation is also seen in the A and B signals to a lesser extent. The inverse relationship of the drift between the C and D signals suggests that the cause may be from humidity drift of an imbalance inside the 1:4 splitter used for measurement, which is being investigated.

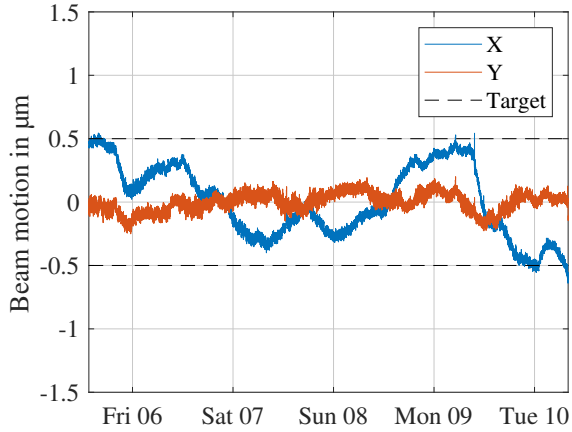

Figure 7: EBPM stability over five days from SA stream data. Target is <1 µm pk-pk long-term requirement.

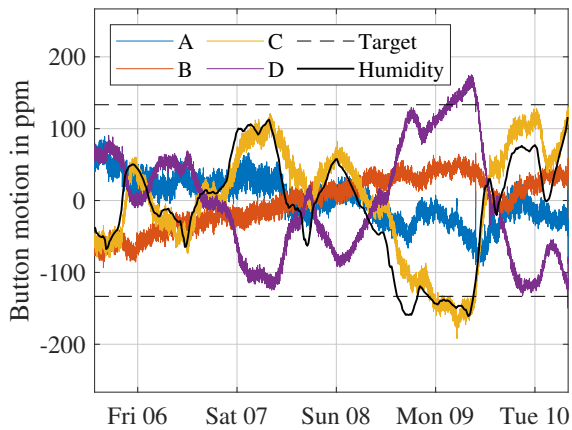

Figure 8: Button signals over five days, showing strong correlation with a local humidity sensor. Humidity is scaled to fit and ranges from 25% to 40% RH. Target is <1 µm pk-pk long-term requirement translated to individual buttons.

CONCLUSION

This paper has presented the new EBPM system for Diamond-II. Although still under development, the current results are encouraging and have validated the design decisions. Next steps include improving long-term stability and investigating software compensation methods for drift.

ACKNOWLEDGEMENTS

The authors wish to thank Dr. Guenther Rehm of Helmholtz-Zentrum Berlin for initial development work on this project.

ISBN: 978-3-95450-241-7 ISSN: 2673-5350 doi:10.18429/JACoW-IBIC2022-MO3C2

REFERENCES

[1] "Diamond-II conceptual design report," Diamond Light Source Ltd., Tech. Rep., 2019. https://www.diamond.ac.uk/dam/jcr:ec67b7e1-fb91-4a65-b1ce-f646490b564d/Diamond-IIConceptualDesignReport.pdf

[2] R. Bartolini *et al.*, "Double-double bend achromat cell upgrade at the Diamond Light Source: From design to commissioning," *Phys. Rev. Accel. Beams*, vol. 21, no. 050701, 2018. doi:10.1103/PhysRevAccelBeams.21.050701

[3] K. B. Scheidt, "Newly developed 6mm buttons for the BPMs in the ESRF Low-Emittance-Ring," in *Proc. IBIC'14*, Monterey, CA, USA, 2014, pp. 346–350. https://jacow.org/IBIC2014/papers/TUPF14.pdf

[4] A. Morgan, "Technological review of beam position button design and manufacture," in *Proc. IBIC'19*, Malmö, Sweden, 2019, pp. 448–452. doi:10.18429/JACOW-IBIC2019-WEAO01

[5] G. Rehm and C. Bloomer, "Impact on relative humidity on EBPM readings," in *Proc. DEELS'15*, Barcelona, Spain, 2015. https://indico.cells.es/event/22/contributions/426/

[6] G. Brajnik, S. Carrato, S. Bassanese, G. Cautero, and R. De Monte, "Pilot tone as a key to improving the spatial resolution of eBPMs," *AIP Conf. Proc.*, vol. 1741, no. 1, p. 020 013, 2016. doi:10.1063/1.4952792

[7] G. Brajnik, S. Bassanese, G. Cautero, R. De Monte, M. Ferianis, and G. Rehm, "Reducing current dependence in position measurements of BPM systems by using pilot tone: Quasi-constant power approach," in *Proc. IBIC'18*, Grand Rapids, MI, USA, 2018, pp. 301–303. doi:10.18429/JACOW-IBIC2017-TUPWC09

[8] M. Cargnelutti *et al.*, "Stability tests with pilot-tone based Elettra BPM RF front end and Libera electronics," in *Proc. IBIC'18*, Shanghai, China, 2018, pp. 289–292. doi:10.18429/JACOW-IBIC2018-TUPB13

[9] G. Kube, "BPM Studies in view of PETRA IV," 15th Libera Workshop, Online at Instrumentation Technologies (Slovenia), 2020. https://bib-pubdb1.desy.de/record/452052

[10] A. Holmes-Siedle and L. Adams, "RADFET: A review of the use of metal-oxide-silicon devices as integrating dosimeters," *Int. J. Radiat. Appl. Instrum. Part C*, vol. 28, no. 2, pp. 235–244, 1986. doi:10.1016/1359-0197(86)90134-7